Time Domain Characterization of Multichip Module Elements

Wolfgang Dressel, Tobias Mangold, Larissa Vietzorreck, *Member, IEEE* and Peter Russer, *Fellow, IEEE*

Institut für Hochfrequenztechnik, Technische Universität München
Arcisstr. 21, D-80333 Munich, Germany, eMail: dressel@hft.ei.tum.de

Abstract— **The development of multichip modules (MCM) or multichip packages (MCP) is an important step towards the miniaturization of integrated circuits. In this technique two or more chips without housing are mounted on a single substrate and connected by each other, resulting in very small and compact elements. An important role for the quality of this modular concept is the performance of the connecting structures and external devices like DC-blocks or line crossings between the ICs. In this contribution various elements will be analysed by the TLM method. A deembedding technique for the S-parameter calculation is presented and windowing functions for the time-domain signals are investigated in order to decrease the computation time. Results are demonstrated for S-parameters of interdigital capacitors and a balun transformer compared to measurements.**

I. INTRODUCTION

In multichip modules (MCM) several chips are mounted together on a carrier substrate to increase density, improve system performance and reduce costs. This integration technique allows combinations of different material systems like gallium arsenide and silicon in the same application. For the connection of the chips different technologies are available: bond wires, flip chip or the insertion of the chip into the substrate by an epoxy adhesive. The commonly used bond wires or flip chips are cost-effective and space-saving, respectively [1], [2]. However, for higher frequencies the discontinuities in the signal path caused by those transition interconnects become more severe, resulting in partial loss, reflection and possibly distortion of the signal [3]. All these issues need to be considered in the design of the package.

In the MCM elements under investigation [4], [5] another technique is used, where the chip is directly inserted into the substrate and fixed by an adhesive. In fig. 1 the transition of a microstrip line to a chip is depicted. The microstrip is first matched to a coplanar line. A coplanar line on the embedded chip is then connected with this coplanar line on the carrier substrate. The transition between the coplanar line and the microstrip line has to be optimized for minimum reflection and minimum losses within the frequency band from 600 MHz to 50 GHz. As the thermal expansion of the adhesive can destroy the signal layer, an additional polymer is applied on the gap between adhesive and signal path. For the manufacture of such transitions normal thin film processes common in the semiconductor industry are used. In this way low-cost devices can be produced.

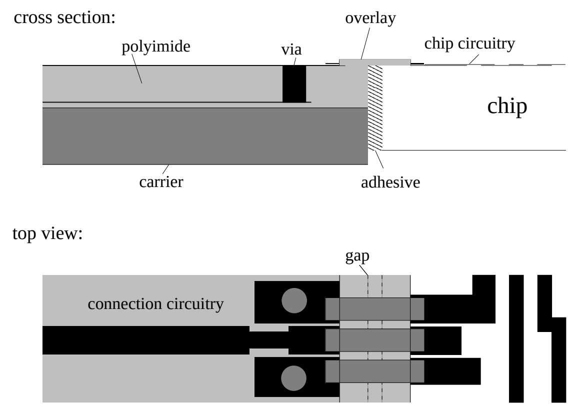

Fig. 1. Schematic view of a MCM interconnection, cross section and top view

In order to investigate the features of the above described elements, a multilayered structure has to be calculated accurately. Here the layered structure consists of a 635 μm Al_2O_3 carrier, a 5 μm Cu ground layer, a 25 μm Polyimide (PI-2722 from Du Pont) layer and a 5 μm Cu signal layer. In this contribution the TLM method is used for the numerical characterization of the MCM structures. The time domain method gives accurate results using less memory than frequency domain methods. Three-dimensional structures can be modeled without difficulties, including losses in substrate and metallization. Depending on the structures long computation times in time-domain can occur. An abrupt truncation of the time domain signal will lead to severe deviations in frequency domain. The deviations can be reduced using suitable windowing functions. Another problem is the reflection of the outgoing waves at the non-perfect port terminations. This problem can be solved applying a deembedding technique. The simulated results are always compared to measurements of the structures under investigation in order to validate the numerical results.

II. TLM SIMULATION AND MEASUREMENTS

In the following TLM simulation results will be presented for an interdigital capacitor, depicted in fig. 2. The used

TLM discretization and the number of nodes are shown in this figure, too.

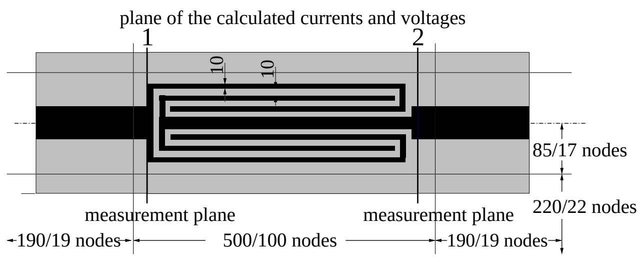

Fig. 2. Interdigital capacitor with dimensions (in μm) and number of nodes

The simulation was performed using 5 μm as smallest mesh size and 10 μm as longest mesh size. Furthermore the 5 μm thick Cu-layers were modeled with finite conductivity of 5.8e7 Sm^{-1}. The S-parameters are calculated from the computed generalized port currents or voltages obtained by path integrals in measurement cross section. In this way we obtain for example S_{11} from the incident generalized voltage wave amplitude V_{Ref} and the resulting generalized input port voltage V_1 via

$$S_{11}(f) = \pm \frac{V_1 - V_{Ref}}{V_{Ref}} \tag{1}$$

In this formula either the corresponding voltages or currents (with the minus) obtained from the integrals can be used for V_1 and V_{Ref}. A comparison between the scattering parameters calculated by TLM and measured values shows a very good coincidence as it can be seen in fig. 3 for S_{11}. The deviation is max. 1 dB.

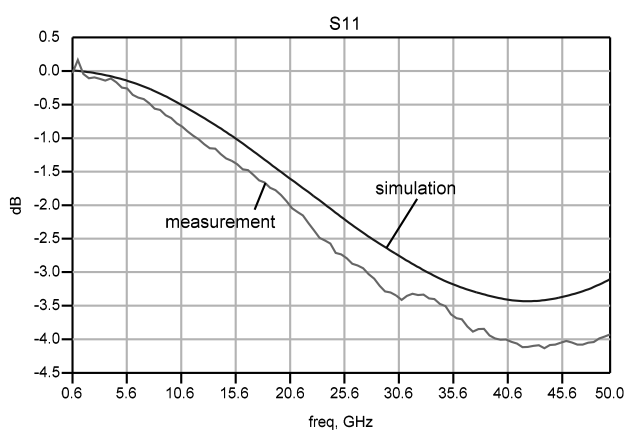

Fig. 3. Simulated and measured S_{11} and S_{21} of the above shown interdigital capacitor

The measurements were performed using a HP 8510C network analyzer and a Cascade on-wafer prober. With the used cell sizes the computation time took 3 hours on a HP-C360 workstation with 500MB memory. The computation time includes the two needed device simulations, and the reference simulation for the incident generalized voltage wave amplitude V_{Ref} needed for the S-parameter calculation.
A problem in time domain modelling is the truncation of the simulated signals. Different strategies are possible to avoid errors caused by an abrupt truncation of the signal. Windowing of the signal [7] or an analytic prolongation using Pencil of Function or Prony-method [8] can be applied to the time domain signal. In the following examples a Hanning window was used in the time domain to improve the frequency domain results. Fig. 5 shows S_{11} of the interdigital capacitor with straight fingers depicted in fig. 4.

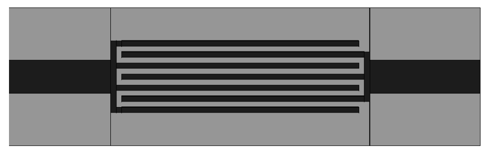

Fig. 4. An interdigital capacitor with straight fingers

The S-parameters are computed from impulse responses of different simulation length - 30000, 500000 timesteps and the same 30000 timesteps-simulation windowed by a Hanning-window in the time domain.

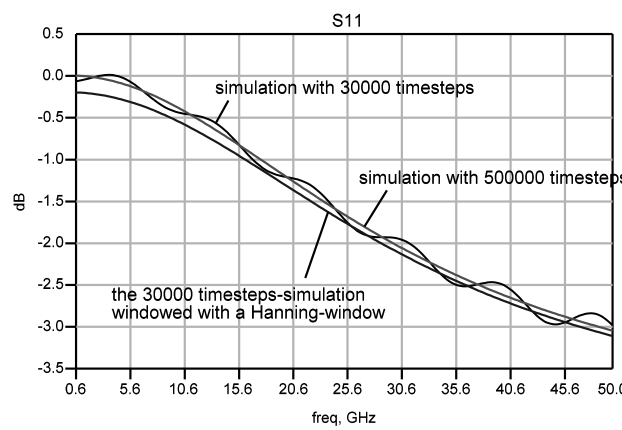

Fig. 5. A 30000 timesteps simulation windowed and not windowed in comparison to a 500000 timesteps simulation

As it can be seen in fig. 5, the S-parameter curve of the simulation with 30000 timesteps shows some ripples compared to the much longer simulation with 500000 timesteps. The reason for this is a too short simulation time. The artificial truncation of impulse responses can be expressed by a multiplication of the infinite time domain signal with a rectangular window. This rectangular windowing causes then the ripple in the frequency domain. To suppress these ripples the impulse response can be multiplied by window functions commonly used in signal processing. The final signal obtained by this operation can be written as follows, if the infinite impulse response is termed with $s(t)$, the rectangular window with $r(t)$ and the used window with $w(t)$:

$$s(t)r(t)w(t) \quad \circ\!\!-\!\!\bullet \quad S(f) * R(f) * W(f) \qquad (2)$$

The best results were obtained with a Hanning window, which is described by eq. 3.

$$w(t) = \begin{cases} 0.5\left(1+\cos\left(2\pi\frac{t}{T}\right)\right) & : \quad |t| < \frac{T}{2} \\ 0 & : \quad \text{otherwise} \end{cases} \qquad (3)$$

The balun transformer depicted in fig. 6 is an example of a more complicated structure.

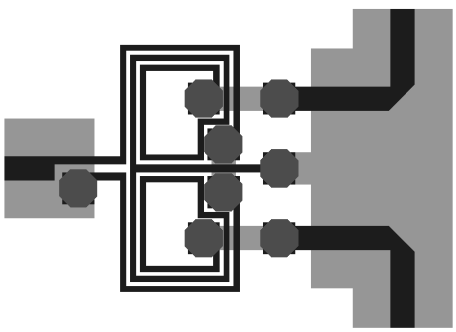

Fig. 6. A balun in microstrip-technique

Fig. 7 shows the measured and calculated S-parameters of this balun transformer. In this example the impedance boundary walls as termination of the ports caused some reflections, which yield to erroneous S-parameters. One method to avoid these reflections is the deembedding technique described in the following.

Let $\mathbf{a}_1$, $\mathbf{a}_2$, ... $\mathbf{a}_N$ be the vectors describing the excitation in the first, second and N^{th} simulation, and let $\mathbf{b}_1$, $\mathbf{b}_2$, ... $\mathbf{b}_N$ denominate the vectors summarizing the scattered waves. We then may introduce the $N \times N$ matrices

$$\mathbf{A} = [\mathbf{a}_1, \mathbf{a}_2, \ldots, \mathbf{a}_N] \ , \qquad (4)$$

$$\mathbf{B} = [\mathbf{b}_1, \mathbf{b}_2, \ldots, \mathbf{b}_N] \ . \qquad (5)$$

A number of N simulations is carried out, where in the i–th simulation, (i = 1 . . . N) a primary pulse wave a_{0i} is applied to the i–th port. The ports of the multiport are terminated with

the reflection factors $\rho_1, \rho_2, \ldots \rho_N$. The waves flowing into the multiport are given by

$$\mathbf{A} = \mathbf{A_0} + \mathbf{\Gamma}\,\mathbf{B} \ , \qquad (6)$$

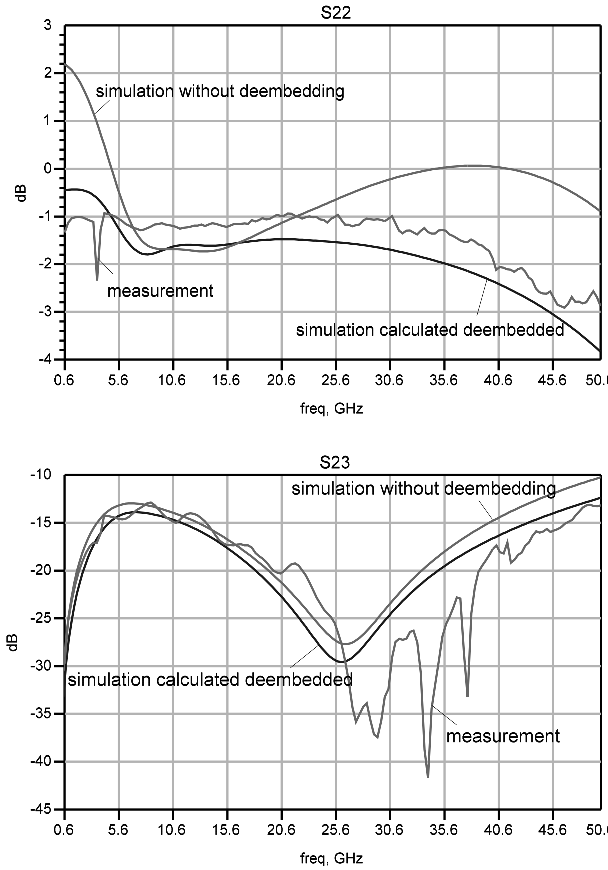

Fig. 7. Simulated and measured S_{22} and S_{23} and S_{13} of the balun

with $\mathbf{\Gamma} = diag\,[\rho_1, \rho_2, \ldots, \rho_N]$. If $\mathbf{A}^{-1}$ exists, the scattering matrix of the multiport can be obtained from

$$\mathbf{S} = \mathbf{B}\,\mathbf{A}^{-1} \qquad (7)$$

For this evaluation both, $\mathbf{A}$ and $\mathbf{B}$ have to be known. This procedure yields a deembedding of non–perfectly terminated multiports.

Fig. 7 shows selected S-parameters of the depicted balun above derived by the conventional method according to eq. (1), the deembedding method after eq. (7) and the measurement. Note that S_{22} yields unphysical values above 0 dB at lower frequencies, when it is calculated by the conventional method. Using the deembedding technique for the calculation a good coincidence with the measured values is obtained. For the other S-parameter the differences between the two calculating methods are not as significant as for the reflection coefficient S_{22}. The simulation time amounts to 14 hours for the three device simulations and the reference simulation.

At last the distribution of the E_z field component of the balun is mapped in fig. 8. It shows the intensity of the E_z component in the plane between the two metal layers.

The two opposite polarisations of the outgoing waves can be clearly observed.

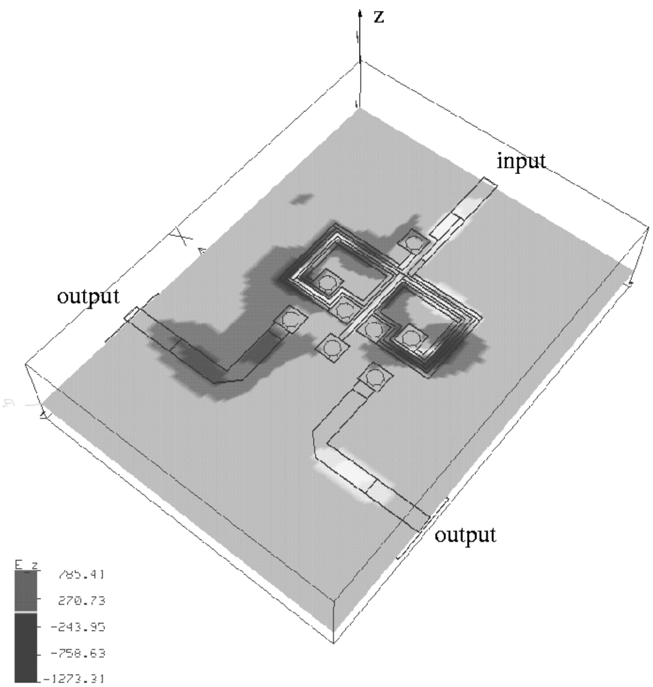

Fig. 8. The E_z field intensity in the plane between the two metal layers of the microstrip

III. Conclusion

In this work the suitability of the TLM method for an efficient and accurate analysis of complex multilayered structures has been demonstrated. The method has been applied to interconnects and other passive elements used for the connection of multichip modules. For the simulation of an interdigital capacitor details were discussed, how to analyze the given structure with high accuracy and to reduce the computation time. In a further example a deembedding technique was introduced and applied to the S-parameter calculation of a balun transformer. The results of the computation were compared with measurements. A good coincidence between the simulated and measured results can be stated for all examples.

Acknowledgement

The authors would like to thank T. Mangold for the implementation of the TLM code and the helpful discussions.

References

[1] W. Heinrich, A. Jentzsch and G.Baumann, Millimeterwave characteristics of flip-chip interconnects for multi-chip modules, IEEE Trans. on Microwave Theory and Techniques, vol. 46, no. 12, December 1998, pp. 2264-2268.

[2] H. Ghouz and E. El-Sharawy, An accurate equivalent circuit model of flip chip and via interconnects. IEEE Trans. on Microwave Theory and Techniques, vol. 44, no. 12, December 1996, pp. 2543-2554.

[3] P. Russer, “Emerging Technologies in Microwaves, Microelectronics and Hybrid Integration, *Microtec 2000 Conference Digest*, Hannover, September 2000.

[4] T. Mangold, P. Gulde, G. Neumann and P. Russer, “A Multichip Module Integration Technology on Silicon Substrate for High Frequency Applications, *Proc. of topical meeting on ’Silicon Monolithic Integrated Circuits in RF Systems*, Ann Arbor, Michigan,181-184,17.-18 September 1998

[5] T. Mangold, J. Wolf, M. Töpper, H. Reichl and P. Russer, A Multichip Module Integration Technology for High-Speed Analog and Digital Applications, *Proc. ISSSE* ,Pisa(Italy), 91-96, September 1998.

[6] T. Mangold and P. Russer, “Full-Wave Modelling and Automatic Equivalent-Circuit Generation of Millimeter-Wave Planar and Multilayer Structures”, IEEE Trans. on Microwave Theory and Techniques, 47, (6), pp. 851-858, June 1999.

[7] A. Papoulis, Signal analysis, McGraw-Hill, 1989.

[8] F. Coccetti, L. Vietzorreck, V. Chtchekatourov, P. Russer, A Numerical Study of MEMS Capacitive Switches using TLM, *Proc. Applied Computational Electromagneticas Symposium (ACES)*, Monterey, CA, March 20-24, 2000, pp. 580-586.